

# UC Irvine

## UC Irvine Previously Published Works

### Title

Insights into Complex Oxidation during BE-7585A Biosynthesis: Structural Determination and Analysis of the Polyketide Monooxygenase BexE

### Permalink

<https://escholarship.org/uc/item/0b4745tq>

### Journal

ACS Chemical Biology, 11(4)

### ISSN

1554-8929

### Authors

Jackson, David R  
Yu, Xia  
Wang, Guojung  
[et al.](#)

### Publication Date

2016-04-15

### DOI

10.1021/acscchembio.5b00913

Peer reviewed



Published in final edited form as:

*ACS Chem Biol.* 2016 April 15; 11(4): 1137–1147. doi:10.1021/acscchembio.5b00913.

## Insights into Complex Oxidation during BE-7585A Biosynthesis: Structural Determination and Analysis of the Polyketide Monooxygenase BexE

David R. Jackson<sup>†</sup>, Xia Yu<sup>‡</sup>, Guojung Wang<sup>‡</sup>, Avinash Patel<sup>†</sup>, Jordi Calveras<sup>||</sup>, Jesus Barajas, Eita Sasaki<sup>||</sup>, Mikko Metsä-Ketelä<sup>§</sup>, Hung-wen Liu<sup>||</sup>, Jürgen Rohr<sup>†,\*</sup>, and Shiou-Chuan Tsai<sup>†,\*</sup>

<sup>†</sup>Department of Molecular Biology and Biochemistry, Department of Chemistry, and Department of Pharmaceutical Sciences, University of California, Irvine, California 92697, United States

<sup>‡</sup>Department of Pharmaceutical Sciences, College of Pharmacy, University of Kentucky,

Lexington, Kentucky 40536, United States <sup>§</sup>Department of Biochemistry, University of Turku,

20014 Turku, Finland <sup>||</sup>Division of Medicinal Chemistry, College of Pharmacy and Department of Chemistry, University of Texas at Austin, Austin, Texas 78712, United States

### Abstract

Cores of aromatic polyketides are essential for their biological activities. Most type II polyketide synthases (PKSs) biosynthesize these core structures involving the minimal PKS, a PKS-associated ketoreductase (KR) and aromatases/cyclases (ARO/CYCs). Oxygenases (OXYs) are rarely involved. BE-7585A is an anticancer polyketide with an angucyclic core. <sup>13</sup>C isotope labeling experiments suggest that its angucyclic core may arise from an oxidative rearrangement of a linear anthracyclinone. Here, we present the crystal structure and functional analysis of BexE, the oxygenase proposed to catalyze this key oxidative rearrangement step that generates the angucyclinone framework. Biochemical assays using various linear anthracyclinone model compounds combined with docking simulations narrowed down the substrate of BexE to be an immediate precursor of aklaviketone, possibly 12-deoxy-aklaviketone. The structural analysis, docking simulations, and biochemical assays provide insights into the role of BexE in BE-7585A biosynthesis and lay the groundwork for engineering such framework-modifying enzymes in type II PKSs.

### Graphical Abstract

\*Corresponding Authors. Tel.: 859-323-5031. jrohr2@email.uky.edu, Tel.: 949-824-4486. sctsay@uci.edu.

#### ASSOCIATED CONTENT

##### Supporting Information

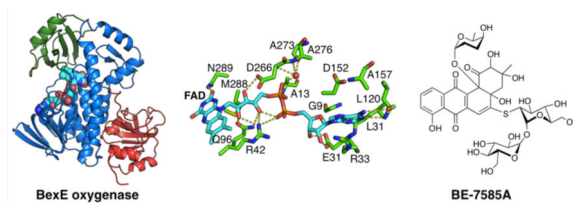
The Supporting Information is available free of charge on the [ACS Publications website](https://pubs.acs.org) at DOI: 10.1021/acscchembio.5b00913.

Three figures and two tables (PDF)

#### Accession Codes

The atomic coordinates of BexE structure has been deposited in the Protein Data Bank (PDB ID: 4X4J).

The authors declare no competing financial interest.



Angucyclines are a diverse group of bioactive natural products produced by type II polyketide synthases (PKSs) that contain modified benz[*a*]anthraquinone cores.<sup>1–3</sup> Many angucyclines have been discovered with anticancer and antibiotic properties such as the urdamycins, landomycins, gaudimycins, oviedomycins, jadomycins, and azicemicins (Figure 1A).<sup>4–9</sup> The biosynthesis of angucyclines has been studied extensively because of their important biological activity and pharmaceutical potential.<sup>3</sup>

Type II polyketides are biosynthesized two carbons at a time from malonyl-CoA building blocks to yield reactive poly- $\beta$ -ketones.<sup>2,3</sup> The reactive poly- $\beta$ -ketone intermediates are regioselectively reduced, cyclized, and aromatized by ketoreductases (KRs), cyclases (CYCs), and aromatase/cyclases (ARO/CYCs), respectively.<sup>3,10</sup> These initial enzymatic transformations yield polycyclic aromatic intermediates, which then undergo a variety of tailoring reactions that include, but are not limited to, oxidation, methylation, reduction, dehydration, and glycosylation.<sup>11</sup> Tailoring enzymes are nature's tools to diversify type II polyketide biosynthesis. Many type II PKS products share common cores, and different combinations of tailoring enzymes modify these core molecules to yield diverse final products with anticancer, antibiotic, and antiviral activities.<sup>10,11</sup> For example, the widely used anticancer drugs daunorubicin and doxorubicin are both hydroxylated and glycosylated during biosynthesis; these modifications are critical for their bioactivity.<sup>12</sup> Tailoring enzymes often use structurally complex and unstable substrates, which are formed transiently during biosynthesis.<sup>6</sup> Therefore, structural and functional characterization of these enzymes, their substrates, and ensuing products is highly challenging.

The oxygenase BexE is involved in an uncharacterized oxidation step during BE-7585A biosynthesis.<sup>13</sup> BE-7585A is an angucyclic polyketide with anticancer properties that was isolated from *Amycolotopsis orientalis* sp. *vinerea*.<sup>13</sup> Because of its complex structure, BE-7585A has inspired multiple biosynthetic studies.<sup>13–15</sup> Previous <sup>13</sup>C isotope labeling experiments suggest that during BE-7585A biosynthesis, a linear tetracyclic intermediate is initially formed, then undergoes an oxidative rearrangement to yield an angucycline (Figure 1B).<sup>13</sup> Our current work suggests that the BexE substrate is a linear tetracyclic intermediate that is different from the originally proposed intermediate shown in Figure 1B. The BE-7585A gene cluster contains three candidate oxygenase genes, BexE, BexI, and BexM, which are proposed to catalyze oxidative tailoring of the BE-7585A aglycone core.<sup>13</sup> Based on protein sequence similarity, BexE is most similar to aromatic hydroxylases that oxidize angucyclines. Elucidating the structure and function of BexE will help to understand an intriguing oxidative tailoring event that is involved in transforming an anthracycline to an angucycline core. Given the large number of known angucycline and anthracycline pathways, this knowledge will pave the way for alternative engineering routes to bioactive metabolites of either the angucycline or the anthracycline class of type II polyketides.

Here, we present the crystal structure of BexE bound to FAD, molecular docking of proposed substrates, and *in vitro* functional studies. In a critical comparison of BexE with RdmE, a biosynthetic FAD-dependent oxygenase is also presented. These results offer the first insight into oxidative tailoring during BE-7585A biosynthesis and provide a basis for engineering oxidation during type II polyketide biosynthesis to yield new bioactive molecules.

## RESULTS AND DISCUSSION

### Overall Structure of BexE

BexE crystallized in the space group C2 with two BexE molecules per asymmetric unit. The BexE dimer is composed of two monomers related by a noncrystallographic 2-fold rotational axis of symmetry (Figure 2A). The protein–protein interface between monomers is moderate with a surface area estimated to be 922.7 Å<sup>2</sup> (PISA).<sup>16</sup> Both monomers are nearly identical and when overlaid, the overall RMSD is 0.241 Å. Each monomer contains an FAD binding domain (Met1–Thr169 and Thr259–Gly372), a middle domain (Ala170–Ala258), and a C-terminal domain (Leu373–Arg487; Figure 2B). This domain arrangement is in agreement with other structurally characterized members of the para-hydroxybenzoate hydroxylase (pHBH) superfamily, including related type II polyketide and alkaloid monooxygenases (Figures S1 and S2; Table S1).<sup>17–22</sup> The FAD binding domain consists of 10  $\alpha$ -helices ( $\alpha$ 1– $\alpha$ 6 and  $\alpha$ 8– $\alpha$ 10) and 10  $\beta$ -sheets ( $\beta$ 1– $\beta$ 9 and  $\beta$ 14) that are connected by a series of 18 loops (L1–L13 and L18–L22). FAD is bound almost entirely in the FAD binding domain, while only contacting the middle domain by hydrophobic interactions with the 1,2-dimethyl moiety of the isoalloxazine ring (Figure 2B). The middle domain is inserted between  $\alpha$ 6 and  $\beta$ 14 of the FAD binding domain. The middle domain consists of one  $\alpha$ -helix ( $\alpha$ 7) and four  $\beta$ -sheets ( $\beta$ 10– $\beta$ 13) that are connected by a series of four loops (L14–L17). The middle domain has been implicated in substrate binding and, in some cases, undergoes structural rearrangements during substrate binding and product release.<sup>19,21–25</sup> In BexE, a large pocket is located adjacent to the isoalloxazine ring of FAD, which is formed between the FAD binding domain and the middle domain. This pocket is hypothesized to be the substrate binding pocket. The C-terminal domain has a thioredoxin fold but lacks the conserved active site cysteines for thioredoxin activity.<sup>26</sup> Therefore, the C-terminal domain may be important for structural stability of BexE but not for catalytic activity.

### FAD Binding in BexE

FAD consists of three parts: the adenosine (adenine and ribose), riboflavin, and the bridging diphosphates. The adenine ring of FAD is positioned between Arg33 (L3) and Asp152 (L12), which interact with opposite faces of the adenine ring (Figure 2C). Gly9 (L1), Ala157 ( $\alpha$ 6), and Leu31 ( $\beta$ 2) define the adenine-binding site by interacting with the edges of the adenine ring. Arg33 forms a hydrogen bond with N7 of adenine while the Leu120 ( $\beta$ 6) amide NH and carbonyl form hydrogen bonds with the N1 of adenine and amine group at the C6 position. The ribose ring of FAD is anchored tightly in place by Glu32 ( $\beta$ 2), which forms hydrogen bonds to the 2' and 3' hydroxyl groups. The first phosphate, moving from the adenosine toward the isoalloxazine ring, forms an intramolecular hydrogen bond with the riboflavin hydroxyl group. This phosphate also forms a weak hydrogen bond with

Arg42. The second phosphate forms a hydrogen bond with the amide NH of Ala13 ( $\alpha$ 1) and also a water molecule, which is held in place by the Ala273 ( $\beta$ 14) carbonyl oxygen and Ala276 (L19) amide NH. The three hydroxyl groups of the riboflavin form hydrogen bonds with Arg42 (L3), Gln96 ( $\alpha$ 5), and Asp275 (L19). The isoalloxazine is positioned between the C-terminal end of  $\alpha$ 8, loops L3 and L9, and  $\beta$ 10 and  $\beta$ 13. L3 and L9 interact with opposite faces of the isoalloxazine ring, while  $\beta$ 10 and  $\beta$ 13 make hydrophobic contacts with the dimethyl moiety. The C2 carbonyl oxygen of the isoalloxazine ring forms hydrogen bonds with the Asn289 ( $\alpha$ 8) side chain and M288 ( $\alpha$ 8) amide NH. FAD coelutes with BexE during purification, and this supports that the cofactor is tightly bound to the enzyme.

### The Role of FAD in BexE and Related Oxygenases

Many oxygenase enzymes, such as BexE, employ FAD for redox-based catalysis.<sup>27</sup> For NAD(P)H dependent enzymes, the FAD cofactor is reduced by NAD(P)H and then reacts with molecular oxygen to form a highly reactive oxygen species at the C4a position of the isoalloxazine ring. FAD reduction is proposed to occur when the isoalloxazine ring of FAD is flipped away from the active site and toward the solvent. This outward conformation of FAD is termed the “out” conformation.<sup>28</sup> Once FAD is reduced by NAD(P)H, the isoalloxazine moves back into the active site pocket, where oxidation of the cofactor and subsequent oxidation of the substrate is proposed to occur. When the FAD moiety is positioned inward toward the active site pocket, the conformation is the “in” conformation. Multiple crystal structures of FAD/NAD(P)H-dependent oxygenases have been solved with FAD in either the “in” or “out” conformations (Figure S1; Table S1).<sup>6,17,19,21–25</sup> A subset of these structures has a substrate bound that allows the identification of substrate binding pockets, as well as the relative locations between FAD and the bound substrate.<sup>19,22</sup> In summary, while homologous oxygenases have been crystallized with FAD in the “in” conformation or “out” conformations, the BexE FAD is in the “in” conformation with a large open active site pocket (Table S1).

### Studies to Identify the BexE Substrate Using *in Vitro* Functional Assays

To determine the substrate and product of the reaction catalyzed by BexE, we tested the ability of BexE to oxidize linear and angular tetracyclic polyketides (Figure 3A). *In vitro* assays were conducted with an NADPH regeneration system and included BexF, which is a putative fourth ring cyclase. Initial BexE assays in the presence of NADPH using possible linear tetracyclic substrates such as presteffimycinone, premithramycinone, aklaviketone, and a fully aromatic shunt product methyl 2-ethyl-4,5,7-trihydroxy-6,11-dioxo-6,11-dihydrotetracene-1-carboxylate (dehydro-aklaviketone)<sup>29</sup> did not lead to product formation (Figure 3A,B). Additionally, assays testing the reversibility of BexE using possible angular tetracyclic substrates such as landomycinone, 11-deoxy-landomycinone, tetrangulol, and tetrangomycin in the presence of NADP<sup>+</sup> showed no product formation (Figure 3A). However, new products were observed when BexE was incubated in the presence of NADPH with the crude lysate from *Streptomyces galilaeus* (ATCC 31615) mutant H036, which produces aklaviketone and the dehydro-aklaviketone (Figure 3B,C).<sup>30</sup> The crude lysate predominantly contains aklaviketone and dehydro-aklaviketone; however, there are also many unstable and uncharacterized biosynthetic intermediates *en route* to these products in the lysate. To identify the true BexE substrate, the crude lysate was

fractionated, and individual fractions were tested for activity with BexE (Figure 3C). A single peak present in “fraction 2” was converted into two new products when incubated with BexE. Interestingly, the unknown BexE substrate accumulates in the crude lysate over time and reaches a maximum amount after 5 h at RT. Due to the instability of the substrate and products, scaling up the BexE *in vitro* reaction for structure elucidation has proved difficult. In summary, we have developed an *in vitro* functional assay for BexE using the crude lysate of *Streptomyces galilaeus* (ATCC 31615) mutant H036, which produces aklaviketone. The lysate contains an uncharacterized product that is most likely a shunt product or biosynthetic intermediate, which is produced during aklaviketone biosynthesis.

### The Effect of BexF During the BexE *in Vitro* Assay

BexF is the proposed fourth cyclase during BE-7885A biosynthesis and shares 39% identity to TcmI, the fourth ring cyclase during tetracenomycin biosynthesis (Figure 4A).<sup>31,32</sup> BexF is proposed to catalyze cyclization(s) immediately before the BexE-catalyzed oxidation during BE-7585A biosynthesis; however, the substrate and product of BexF are unknown. The addition of BexF to the lysate resulted in an increase in the size of the peak at 10.42 min. The addition of BexE and BexF to the lysate resulted in the appearance of the same two new peaks at 19.11 and 24.98 min, which were present with BexE alone. However, when BexF and BexE are present, the peaks at 19.11 and 24.98 min are increased relative to BexE alone (Figure 3B). Therefore, BexF may affect BexE product formation through a number of possible mechanisms. For example, we hypothesize that BexF is involved in the generation or stabilization of the BexE substrate. Alternatively, BexF may form a complex with BexE and alter the kinetics of the BexE reaction, or help shuttle a reactive substrate into the BexE active site. The observation that the inclusion of BexF increases BexE product formation strongly supports that these two enzymes, a cyclase and an oxygenase, associate together.

### Possible BexF and BexE Substrates

Based on our *in vitro* assay results, the BexE substrate in the crude lysate of *Streptomyces galilaeus* (ATCC 31615) mutant H036 is neither aklaviketone nor dehydro-aklaviketone. Therefore, the BexF or BexE substrate is possibly either a linear tricyclic compound such as aklanonic acid, aklanonic acid methyl ester, 12-deoxy-aklanonic acid, or a linear tetracyclic substrate such as aklaviketonic acid or 12-deoxy-aklaviketonic acid (Figure 4B). Because of the unavailability or instability of the proposed substrates, the unaromatized intermediates shown in Figure 4B could not be tested *in vitro*. However, we are exploring compounds such as aklanonic acid and aklanonic acid methyl ester as BexF or BexE substrates. 12-Deoxy-aklanonic acid and 12-deoxy-aklanonic acid methyl ester are prone to oxidation at the C12 position; therefore, these compounds may not be stable over long periods of time. However, during biosynthesis, 12-deoxy-aklanonic acid derivatives may be stabilized by sequestration into an enzyme active site or binding pocket, which could protect the C12 position from oxidation. The protected 12-deoxy-aklanonic acid could then be shuttled directly into the correct active site for catalysis. BexF may catalyze fourth ring formation of 12-deoxy-aklanonic acid to form 12-deoxy-aklaviketonic acid, which we hypothesize to be the BexE substrate.

The presence or absence of the methyl ester at C10 may also influence activity. The C10 carboxy methyl ester is important for the cyclization of aklanonic acid methyl ester to form aklaviketone by the cyclase DnrD in daunorubicin biosynthesis.<sup>29,33</sup> Therefore, the C10 carboxylate may be an important determinant of substrate specificity for BexE.

Another possible determinant of substrate specificity is the stereochemistry at the C9 position. During aklaviketone biosynthesis in *Streptomyces galilaeus* (ATCC 31615), the stereochemistry at the C9 position is set during the enzyme-catalyzed cyclization of aklanonic acid methyl ester.<sup>29</sup> However, aklanonic or 12-deoxy-aklanonic acid may undergo spontaneous decarboxylation, resulting in the formation of a carbanion at the C10 position. The reactive C10 carbanion is poised to form a six-membered ring by attacking the C9 carbonyl. This reaction would produce equal mixture of stereoisomers at the C9 position. It is possible that spontaneous decarboxylation occurs, which leads to the formation of the BexE substrate with different stereochemistry than aklaviketone. BexF may increase the rate of decarboxylation/cyclization of aklanonic or 12-deoxy-aklanonic acid, and thus it would likely favor one stereoisomer over the other. This scenario could explain the increase in product formation when BexF is present in the assay with crude lysate.

In summary, we have found that BexE can convert a to-be-determined substrate from the crude lysate of *Streptomyces galilaeus* (ATCC 31615) into two unknown products in an NADPH-dependent reaction. *Streptomyces galilaeus* (ATCC 31615) produces aklaviketone; therefore, we proposed a series of candidate BexE substrates that are expected to be intermediates during aklaviketone biosynthesis.

### BexF Homology Model Active Site Docking

BexF is likely to produce the BexE substrate. To gain more information about the possible structure of the BexE substrate, we investigated possible substrates and products of BexF using molecular docking with the BexF homology model (Figure 5). A homology model of BexF was generated using HHPred based on the TcmI crystal structure.<sup>34</sup> Linear tricyclic and tetracyclic polyketide intermediates were docked into the BexF model to reveal the impact of C9 stereochemistry, C12 oxidation, and the C10 carboxyl group on substrate binding in the active site. In total, over 500 docking solutions were analyzed for different possible BexF substrates and products. 12-Deoxy-aklaviketonic acid, a putative BexF product, showed the most favorable interactions with BexF (Figure 5A). These preliminary docking results suggest that 12-deoxy-aklaviketonic acid is a possible BexF product; however, aklaviketonic acid or a different linear tetracyclic intermediate may be the true product.

### BexE Active Site Docking

To determine the potential substrate for BexE, multiple tetracyclic intermediates were docked into the BexE active site near FAD. Similar to BexF, 12-deoxy-aklaviketonic acid docked well into the BexE active site (Figure 5B). The tetracyclic structure of 12-deoxy-aklaviketonic acid stacks on the backbone of L3 and forms a series of hydrogen bonds and hydrophobic interactions with BexE (Figure 5B). The BexE substrate pocket is sufficiently large to accommodate a range of tetracyclic molecules. However, upon substrate binding, we



hypothesize that the middle domain undergoes a conformational change, which seals the substrate in the active site. We are currently scaling up the fractionation of the *Streptomyces galilaeus* (ATCC 31615) lysate to generate enough BexE substrate for cocrystallization studies. A BexE cocrystal structure with the true substrate will shed light on the nature of conformational changes upon substrate binding and reveal structural information about the substrate. In summary, docking results of BexE with 12-deoxy-aklaviketononic acid support our hypothesis that 12-deoxy-aklaviketononic acid may be the BexE substrate.

### Docking a BexF Homology Model with BexE

To visualize a possible BexE/BexF complex, the homology model of BexF generated using HHPred based on the TcmI crystal structure was docked with BexE using COOT.<sup>34,35</sup> The docked BexE/BexF complex was further energy minimized using Chimera.<sup>36</sup> The BexF homology model has a large open active site and wide entrance capable of binding linear and angular tetracyclic polyketides. The BexF model was docked with the BexE structure in an orientation that positions their active site entrances in close contact (Figure S3). This orientation mimics a possible binding interaction between BexE and BexF that allows BexF to pass an unstable substrate into the BexE active site. The BexF model binds to the middle domain BexE, which in other related oxygenases can undergo structural rearrangements upon substrate binding.<sup>23</sup> Additionally, there is a large central cavity between the two BexE monomers that may facilitate BexF docking by providing a large interface for interaction. It is possible that BexF protects and shuttles a reactive intermediate to the BexE active site, and structural rearrangements in the middle domain of BexE occur during complex formation with BexF. In summary, we propose that a BexE/BexF complex may form that connects the active site entrances of BexF and BexE to facilitate transfer of a reactive product from BexF to BexE, although further studies are needed to validate this hypothesis.

### Comparison with RdmE

BexE is structurally similar to polyketide hydroxylase RdmE with an RMSD 3.10 Å. Their overall sequence identity is 31%, and we hypothesize that the BexE substrate is similar to the RdmE substrate, aklavinone. RdmE is an FAD/NADPH-dependent polyketide monooxygenase that is responsible for hydroxylation at the C11 position of aklavinone to form  $\epsilon$ -rhodomycinone, which is a precursor to daunorubicin and many other type II PKSs natural products (Figure S1).<sup>19</sup> Aklavinone, the substrate of RdmE, is structurally related to the proposed BexE substrate (Figure 1; Figure S1). The cocrystal structure of RdmE bound to its substrate aklavinone and FAD was determined (Figure 6).<sup>19</sup> The RdmE cocrystal structure reveals the aklavinone binding site with FAD in the “out” conformation. The middle domain of RdmE closes down over the substrate and effectively seals the substrate into a cavity. BexE has a large open active site leading directly into the FAD binding pocket. In contrast, the same region of RdmE, which corresponds to the BexE active site entrance, is completely blocked while the substrate is enclosed inside the pocket (Figure 6). BexE and RdmE may have different active site pocket entrances; however, the middle domain forms both pockets. This allows us to examine the relationship between substrate binding in the middle domain and the “in” and “out” conformations of FAD more comprehensively.



The RdmE crystal structure suggests that upon substrate binding, the FAD moves from the “in” position to the “out” position (Figure 6; Figure 7). In other related oxygenase structures in the absence of substrate, FAD is in the “in” position.<sup>6,25</sup> This is a reasonable hypothesis, because when FAD is reduced in the “out” position, the reduced FAD reacts with molecular oxygen to generate a peroxy-flavin intermediate. Peroxy-flavin intermediates are unstable, and without a substrate to oxidize, the peroxy-flavin will decay. If substrate binding does not control the position of FAD and peroxy-flavin generation, NADPH is needlessly consumed.<sup>37</sup> A model for substrate binding, peroxy-flavin binding, and conformation changes in the middle domain is proposed in Figure 7. In summary, BexE and RdmE may have similar substrates. Based on the RdmE crystal structure bound to aklavinone, we hypothesize that the BexE substrate will bind in an active site pocket formed by the middle domain. Additionally, upon substrate binding, the FAD will move from the “in” position to the “out” position for reduction and subsequent peroxy-flavin generation.

## Conclusions

The crystal structure of the oxygenase BexE was solved to 2.65 Å. It reveals a large active site pocket adjacent to the FAD cofactor, which is positioned in the “in” conformation that has been observed for other FAD/NADPH oxygenase crystal structures in the absence of substrate. Because BexE is part of a large number of enzymes involved in BE-7585A biosynthesis, the identification of its true substrate is a challenging task. Attempts at developing a BexE functional assay with late-stage tetracyclic type II PKS intermediates eliminated many potential BexE substrates and helped establish the substrate tolerance of BexE. Additionally, contrary to other oxygenases, we found that BexE cannot catalyze a reverse reaction using angucyclic polyketides, at least not using the angucyclinones shown in Figure 3A, which supports the unique activity of BexE. We did observe NADPH-dependent BexE activity when BexE was incubated with the lysate of *Streptomyces galilaeus* (ATCC 31615), which produces aklaviketone. The *Streptomyces galilaeus* (ATCC 31615) lysate was fractionated and a single peak was identified as the BexE substrate. Importantly, BexF, the putative fourth ring cyclase that is hypothesized to provide the BexE substrate during BE-7585A biosynthesis, was found to increase BexE product formation in our assay. To gain insight into the structure of the BexE substrate, we conducted molecular docking studies on possible biosynthetic intermediates using a homology model of BexF and the crystal structure of BexE. Our docking results suggest that the substrate of BexE may be 12-deoxy-aklaviketonic acid. We are actively pursuing structural determination of the BexE substrate and products. Comparison of BexE with the related type II PKS oxygenase RdmE also supported docking calculation and provided further insights into how substrate binding may induce conformation changes in the middle domain and regulate catalysis. Together, these results offer an initial glimpse into the complex oxidation reactions that occur during BE-7585A biosynthesis and lay a framework for engineering oxidations in type II PKSs.

## METHODS

### Expression and Purification of BexE

The pET-28b (Novagen) derived DNA plasmid encoding a cleavable N-terminal His-tagged BexE (BexE/pET28b) was provided by Dr. Hung-Wen Liu. BexE/pET28b was transformed

into *E. coli* BL21(DE3) competent cells and plated on LB-agar plates containing kanamycin (50  $\mu\text{g}/\text{mL}$ ). The plates were incubated overnight at 37  $^{\circ}\text{C}$ . A positive transformant was transferred to a 5 mL starter culture of Luria–Bertani (LB) broth containing kanamycin (50  $\mu\text{g}/\text{mL}$ ). The starter culture was grown overnight at 37  $^{\circ}\text{C}$  with shaking. The culture was used to inoculate 2 L of LB with kanamycin (50  $\mu\text{g}/\text{mL}$ ). The culture was grown at 37  $^{\circ}\text{C}$  until the  $A_{600}$  reached 0.4–0.6. The cells were cooled to 18  $^{\circ}\text{C}$ , and 0.1 mM IPTG was added to induce protein expression. After 12–18 h of incubation at 18  $^{\circ}\text{C}$ , the cells were harvested by centrifugation at 5000 rpm for 15 min. The cell pellets were flash-frozen in liquid nitrogen and stored at  $-80^{\circ}\text{C}$ . The frozen cell pellets were thawed on ice and resuspended in lysis buffer (50 mM Tris pH 8.0, 300 mM NaCl, 15% glycerol, 10 mM imidazole). The cell suspension was lysed using sonication ( $8 \times 30$  s cycles), and cell debris was removed by centrifugation at 14 000 rpm for 45 min. The lysate was incubated with 5 mL of Ni-IMAC resin (BioRad) at 4  $^{\circ}\text{C}$  for 1 h. The resin was poured into a fritted column, and the flow-through fraction was collected. The resin was washed with 100 mL of lysis buffer then eluted with lysis buffer plus increasing amounts of imidazole (20–500 mM). The elutions were analyzed using SDS-PAGE, and elutions containing the protein of interest were combined and dialyzed overnight into crystallization buffer (50 mM Tris pH 8.0, 300 mM NaCl, 15% glycerol). The dialyzed protein was concentrated to 5  $\text{mg mL}^{-1}$  and frozen in liquid nitrogen. The appearance of the elutions was bright yellow due to the presence of the FAD cofactor bound to BexE. The theoretical molecular weight of BexE (including the His-tag) is 53 589 Da, which was confirmed using SDS-PAGE.

### BexE Crystallization

Frozen aliquots of BexE were thawed on ice and filtered with a 0.22  $\mu\text{m}$  spin filter prior to crystallization. A total of 1.7  $\mu\text{L}$  of BexE (5  $\text{mg mL}^{-1}$ ) was mixed with 1.7  $\mu\text{L}$  of well solution (30% PEG 3350, 0.2 M ammonium sulfate, 0.1 M MES, pH 4.5) and allowed to equilibrate with 500  $\mu\text{L}$  of well solution using the sitting drop vapor diffusion method. Medium sized clusters containing 3D blades formed over 1 week at 4  $^{\circ}\text{C}$ . The clusters were broken, and single blades were used for diffraction experiments.

### BexE Data Collection, Model building, and Refinement

Crystals of BexE were flash frozen in liquid nitrogen before data collection. X-ray diffraction data using monochromatic X-rays (1.0  $\text{\AA}$ ) were collected for BexE crystals to a resolution of 2.65  $\text{\AA}$  at the Advanced Light Source (ALS) on Beamline 8.2.1. The diffraction data were processed using HKL2000.<sup>38</sup> BexE crystallized as one homodimer per asymmetric unit in the space group *C2*. Initial phases were determined using molecular replacement (PHENIX Phaser) with the structure of the aromatic hydroxylase PgaE (PDB ID: 2QA1) as a search model.<sup>39</sup> A preliminary model was built (PHENIX AutoBuild), and this model was used for iterative rounds of model building (COOT) and refinement (PHENIX refine).<sup>35,40,41</sup> After one round of refinement, clear electron density for the FAD cofactor was observed in both BexE monomers. Once all side chains were correctly placed, FAD was inserted into each monomer and included for all subsequent rounds of model building and refinement. Clear electron density was located near multiple arginines, and three sulfates were modeled and refined in these areas. BexE was refined to yield an  $R_{\text{work}}$  of 19.62% and an  $R_{\text{free}}$  of 24.56%. Data collection and refinement statistics can be found in

Table S2. The following residues could not be confidently placed in the BexE model due to missing electron density: Ile190-Glu192 and Ala445 (monomer A) and Met189-Glu192 and Gly399-Arg401 (monomer B).

### Molecular Docking

Putative substrates for oxidation were drawn using ChemDraw and converted to PDBs using the NCI SMILES converter server (<http://cactus.nci.nih.gov/translate/>). The putative substrate PDB files were energy minimized and converted to .mol2 files using Chimera.<sup>36</sup> The BexF homology model was generated using HHPred based on the crystal structure of TcmI. The BexE and BexF PDBs were converted to .mol2 files, and waters were removed using Chimera. GOLD docking was used to dock the putative substrates in the BexE active site within 15 Å of the FAD C4a carbon.<sup>42</sup> For BexF, substrates were docked within 15 Å of the bottom pocket arginine Arg39. The BexF homology model was docked to BexE using COOT, and the docked complex was energy minimized using Chimera.<sup>35,36</sup>

### Biochemical Assays

For determination of the BexE substrate, the enzyme reactions (100 µL) were carried out with each of the possible substrates or the *Streptomyces galilaeus* crude lysate, containing 50 mM Tris-HCl, at a pH of 7.5, 5 µM BexE or 15 µM BexF or both, together with 1 mM NADH or the NADPH regenerating system (1 mM glucose 6-phosphate, 50 µM NADPH, 5 µM glucose-6-phosphate dehydrogenase). After incubation at 28 °C for 1.5 h, these reactions were terminated by the addition of 100 µL of methanol. Assays without enzymes were used as a control. For the BexE reversibility assays, each of the substrates were incubated with 1 mM NADP<sup>+</sup>, 10 µM BexE, and 50 mM Tris-HCl at a pH of 7.5 at 28 °C for 2 h. Landomycinone was isolated from *Streptomyces cyanogenus* GT3. 11-Deoxy-landomycinone,<sup>43</sup> tetrangulol, and tetrangomycin were isolated from *Streptomyces cyanogen* K62.<sup>44</sup> Presteffimycinone was prepared by enzymatic reactions of 2-hydroxy-nogalonic acid catalyzed by StfX (fourth rings cyclase) and StfT (7-KR) and 2-hydroxy-nogalonic acid. Premithramycinone was isolated from M7D1 mutant of *Streptomyces argillaceus* (ATCC 12956),<sup>45</sup> and aklaviketone and dehydro-aklaviketone were isolated from *Streptomyces galilaeus* (ATCC 31615) mutant H036.<sup>30</sup> All the assays were analyzed by LC-MS (Waters HPLC system, consisting of the 2996 photodiode array detector, the 2695 Separations Module, Micromass ZQ, and a Symmetry C18 5 µm 4.6 × 250 mm column at a flow rate of 0.5 mL min<sup>-1</sup>). UV detection was performed at 430 nm.

### Supplementary Material

Refer to Web version on PubMed Central for supplementary material.

### Acknowledgments

This work was supported by NIGMS R01GM076330 (S.-C.T.), National Institutes of Health GM105977 and CA091901 (J.R.), National Institutes of Health GM040541 and GM035906, and Welch Foundation F-1511 (H.-W.L.).

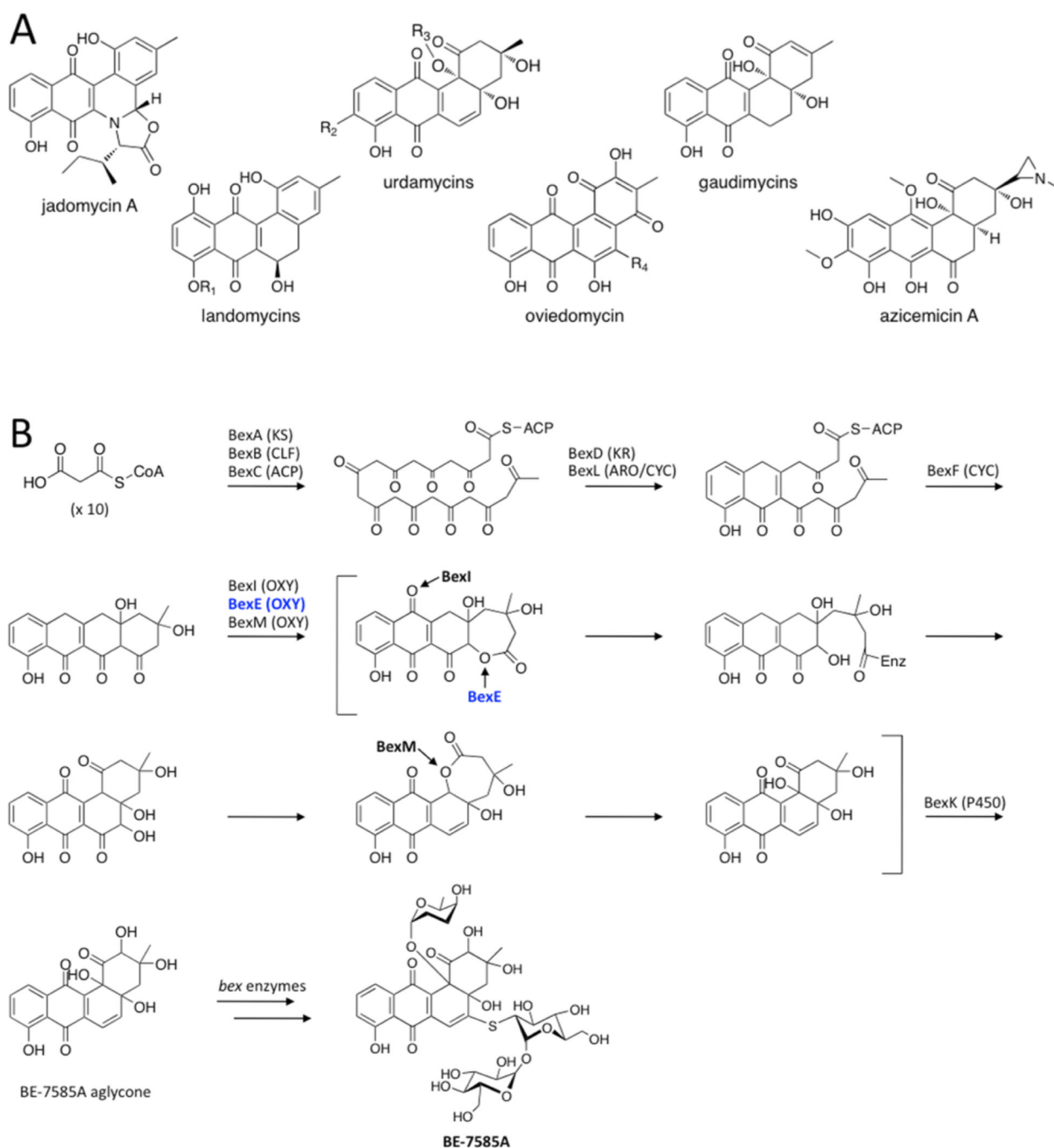
## REFERENCES

1. Metsa-Ketela M, Palmu K, Kunnari T, Ylihonko K, Mantsala P. Engineering anthracycline biosynthesis toward angucyclines. *Antimicrob. Agents Chemother.* 2003; 47:1291–1296. [PubMed: 12654660]
2. Krohn K, Rohr J. Angucyclines: Total syntheses, new structures, and biosynthetic studies of an emerging new class of antibiotics. *Top. Curr. Chem.* 1997; 188:127–195.
3. Kharel MK, Pahari P, Shepherd MD, Tibrewal N, Nybo SE, Shaaban KA, Rohr J. Angucyclines: Biosynthesis, mode-of-action, new natural products, and synthesis. *Nat. Prod. Rep.* 2012; 29:264–325. [PubMed: 22186970]
4. Han L, Yang K, Ramalingam E, Mosher RH, Vining LC. Cloning and characterization of polyketide synthase genes for jadomycin B biosynthesis in *Streptomyces venezuelae* ISP5230. *Microbiology.* 1994; 140(12):3379–3389. [PubMed: 7881555]
5. Henkel T, Rohr J, Beale JM, Schwenen L. Landomycins, new angucycline antibiotics from *Streptomyces* sp. I. Structural studies on landomycins A–D. *J. Antibiot.* 1990; 43:492–503. [PubMed: 2358402]
6. Kallio P, Liu Z, Mantsala P, Niemi J, Metsa-Ketela M. Sequential action of two flavoenzymes, PgaE and PgaM, in angucycline biosynthesis: chemoenzymatic synthesis of gaudimycin C. *Chem. Biol.* 2008; 15:157–166. [PubMed: 18291320]
7. Lombo F, Brana AF, Salas JA, Mendez C. Genetic organization of the biosynthetic gene cluster for the antitumor angucycline oviedomycin in *Streptomyces antibioticus* ATCC 11891. *ChemBioChem.* 2004; 5:1181–1187. [PubMed: 15368568]
8. Ostash B, Korynevskaya A, Stoika R, Fedorenko V. Chemistry and biology of landomycins, an expanding family of polyketide natural products. *Mini-Rev. Med. Chem.* 2009; 9:1040–1051. [PubMed: 19689401]
9. Tsuchida T, Sawa R, Takahashi Y, Inuma H, Sawa T, Naganawa H, Takeuchi T. Azicemicins A and B, new antimicrobial agents produced by *Amycolatopsis*. II. Structure determination. *J. Antibiot.* 1995; 48:1148–1152. [PubMed: 7490223]
10. Hertweck C, Luzhetskyy A, Rebets Y, Bechthold A. Type II polyketide synthases: gaining a deeper insight into enzymatic teamwork. *Nat. Prod. Rep.* 2007; 24:162–190. [PubMed: 17268612]
11. Shen B. Polyketide biosynthesis beyond the type I, II and III polyketide synthase paradigms. *Curr. Opin. Chem. Biol.* 2003; 7:285–295. [PubMed: 12714063]
12. Di Marco A, Cassinelli G, Arcamone F. The discovery of daunorubicin. *Cancer Treat Rep.* 1981; 65(4):3–8. [PubMed: 7049379]
13. Sasaki E, Ogasawara Y, Liu HW. A biosynthetic pathway for BE-7585A, a 2-thiosugar-containing angucycline-type natural product. *J. Am. Chem. Soc.* 2010; 132:7405–7417. [PubMed: 20443562]
14. Sasaki E, Liu HW. Mechanistic studies of the biosynthesis of 2-thiosugar: evidence for the formation of an enzyme-bound 2-ketohexose intermediate in BexX-catalyzed reaction. *J. Am. Chem. Soc.* 2010; 132:15544–15546. [PubMed: 20961106]
15. Sasaki E, Zhang X, Sun HG, Lu MY, Liu TL, Ou A, Li JY, Chen YH, Ealick SE, Liu HW. Co-opting sulphur-carrier proteins from primary metabolic pathways for 2-thiosugar biosynthesis. *Nature.* 2014; 510:427–431. [PubMed: 24814342]
16. Krissinel E, Henrick K. Inference of macro-molecular assemblies from crystalline state. *J. Mol. Biol.* 2007; 372:774–797. [PubMed: 17681537]
17. Koskiniemi H, Metsa-Ketela M, Dobritzsch D, Kallio P, Korhonen H, Mantsala P, Schneider G, Niemi J. Crystal structures of two aromatic hydroxylases involved in the early tailoring steps of angucycline biosynthesis. *J. Mol. Biol.* 2007; 372:633–648. [PubMed: 17669423]
18. Kallio P, Patrikainen P, Belogurov GA, Mantsala P, Yang K, Niemi J, Metsa-Ketela M. Tracing the evolution of angucyclinone monooxygenases: structural determinants for C-12b hydroxylation and substrate inhibition in PgaE. *Biochemistry.* 2013; 52:4507–4516. [PubMed: 23731237]
19. Lindqvist Y, Koskiniemi H, Jansson A, Sandalova T, Schnell R, Liu Z, Mantsala P, Niemi J, Schneider G. Structural basis for substrate recognition and specificity in aklavinone-11-hydroxylase from rhodomycin biosynthesis. *J. Mol. Biol.* 2009; 393:966–977. [PubMed: 19744497]

20. Wang P, Bashiri G, Gao X, Sawaya MR, Tang Y. Uncovering the enzymes that catalyze the final steps in oxytetracycline biosynthesis. *J. Am. Chem. Soc.* 2013; 135:7138–7141. [PubMed: 23621493]
21. Ryan KS, Howard-Jones AR, Hamill MJ, Elliott SJ, Walsh CT, Drennan CL. Crystallographic trapping in the rebeccamycin biosynthetic enzyme RebC. *Proc. Natl. Acad. Sci. U. S. A.* 2007; 104:15311–15316. [PubMed: 17873060]
22. Bosserman MA, Downey T, Noinaj N, Buchanan SK, Rohr J. Molecular insight into substrate recognition and catalysis of Baeyer-Villiger monooxygenase MtmOIV, the key frame-modifying enzyme in the biosynthesis of anticancer agent mithramycin. *ACS Chem. Biol.* 2013; 8:2466–2477. [PubMed: 23992662]
23. Ryan KS, Chakraborty S, Howard-Jones AR, Walsh CT, Ballou DP, Drennan CL. The FAD cofactor of RebC shifts to an IN conformation upon flavin reduction. *Biochemistry.* 2008; 47:13506–13513. [PubMed: 19035832]
24. Goldman PJ, Ryan KS, Hamill MJ, Howard-Jones AR, Walsh CT, Elliott SJ, Drennan CL. An unusual role for a mobile flavin in StaC-like indolocarbazole biosynthetic enzymes. *Chem. Biol.* 2012; 19:855–865. [PubMed: 22840773]
25. Beam MP, Bosserman MA, Noinaj N, Wehenkel M, Rohr J. Crystal structure of Baeyer-Villiger monooxygenase MtmOIV, the key enzyme of the mithramycin biosynthetic pathway. *Biochemistry.* 2009; 48:4476–4487. [PubMed: 19364090]
26. Martin JL. Thioredoxin—a fold for all reasons. *Structure.* 1995; 3:245–250. [PubMed: 7788290]
27. Torres Pazmino DE, Winkler M, Glieder A, Fraaije MW. Monooxygenases as biocatalysts: Classification, mechanistic aspects and biotechnological applications. *J. Biotechnol.* 2010; 146:9–24. [PubMed: 20132846]
28. Brender JR, Dertouzos J, Ballou DP, Massey V, Palfey BA, Entsch B, Steel DG, Gafni A. Conformational dynamics of the isoalloxazine in substrate-free p-hydroxybenzoate hydroxylase: single-molecule studies. *J. Am. Chem. Soc.* 2005; 127:18171–18178. [PubMed: 16366570]
29. Kendrew SG, Katayama K, Deutsch E, Madduri K, Hutchinson CR. DnrD cyclase involved in the biosynthesis of doxorubicin: purification and characterization of the recombinant enzyme. *Biochemistry.* 1999; 38:4794–4799. [PubMed: 10200167]
30. Ylihonko K, Hakala J, Niemi J, Lundell J, Mantsala P. Isolation and characterization of aclacinomycin A-non-producing *Streptomyces galilaeus* (ATCC 31615) mutants. *Microbiology.* 1994; 140(6):1359–1365. [PubMed: 8081501]
31. Thompson TB, Katayama K, Watanabe K, Hutchinson CR, Rayment I. Structural and functional analysis of tetracenomycin F2 cyclase from *Streptomyces glaucescens*. A type II polyketide cyclase. *J. Biol. Chem.* 2004; 279:37956–37963. [PubMed: 15231835]
32. Shen B, Hutchinson CR. Tetracenomycin F2 cyclase: intramolecular aldol condensation in the biosynthesis of tetracenomycin C in *Streptomyces glaucescens*. *Biochemistry.* 1993; 32:11149–11154. [PubMed: 8218177]
33. Kallio P, Sultana A, Niemi J, Mantsala P, Schneider G. Crystal structure of the polyketide cyclase AknH with bound substrate and product analogue: implications for catalytic mechanism and product stereoselectivity. *J. Mol. Biol.* 2006; 357:210–220. [PubMed: 16414075]
34. Soding J, Biegert A, Lupas AN. The HHpred interactive server for protein homology detection and structure prediction. *Nucleic Acids Res.* 2005; 33:W244–W248. [PubMed: 15980461]
35. Emsley P, Cowtan K. Coot: model-building tools for molecular graphics. *Acta Crystallogr., Sect. D. Biol. Crystallogr.* 2004; 60:2126–2132. [PubMed: 15572765]
36. Pettersen EF, Goddard TD, Huang CC, Couch GS, Greenblatt DM, Meng EC, Ferrin TE. UCSF Chimera—a visualization system for exploratory research and analysis. *J. Comput. Chem.* 2004; 25:1605–1612. [PubMed: 15264254]
37. Wang J, Ortiz-Maldonado M, Entsch B, Massey V, Ballou D, Gatti DL. Protein and ligand dynamics in 4-hydroxybenzoate hydroxylase. *Proc. Natl. Acad. Sci. U. S. A.* 2002; 99:608–613. [PubMed: 11805318]
38. Otwinowski Z, Minor W. Processing of X-ray diffraction data collected in oscillation mode. *Methods Enzymol.* 1997; 276:307–326.

39. McCoy AJ, Grosse-Kunstleve RW, Adams PD, Winn MD, Storoni LC, Read RJ. Phaser crystallographic software. *J. Appl. Crystallogr.* 2007; 40:658–674. [PubMed: 19461840]
40. Terwilliger TC, Grosse-Kunstleve RW, Afonine PV, Moriarty NW, Zwart PH, Hung LW, Read RJ, Adams PD. Iterative model building, structure refinement and density modification with the PHENIX AutoBuild wizard. *Acta Crystallogr., Sect. D. Biol. Crystallogr.* 2008; 64:61–69. [PubMed: 18094468]
41. Afonine PV, Grosse-Kunstleve RW, Echols N, Headd JJ, Moriarty NW, Mustyakimov M, Terwilliger TC, Urzhumtsev A, Zwart PH, Adams PD. Towards automated crystallographic structure refinement with phenix.refine. *Acta Crystallogr., Sect. D. Biol. Crystallogr.* 2012; 68:352–367. [PubMed: 22505256]
42. Verdonk ML, Cole JC, Hartshorn MJ, Murray CW, Taylor RD. Improved protein-ligand docking using GOLD. *Proteins: Struct., Funct., Genet.* 2003; 52:609–623. [PubMed: 12910460]
43. Luzhetskyy A, Liu T, Fedoryshyn M, Ostash B, Fedorenko V, Rohr J, Bechthold A. Function of lanGT3, a glycosyltransferase gene involved in landomycin A biosynthesis. *ChemBioChem.* 2004; 5:1567–1570. [PubMed: 15515090]
44. Shaaban KA, Stamatkin C, Damodaran C, Rohr J. 11-Deoxylandomycinone and landomycins X-Z, new cytotoxic angucyclin(on)es from a *Streptomyces cyanogenus* K62 mutant strain. *J. Antibiot.* 2011; 64:141–150. [PubMed: 20978514]
45. Blanco G, Fernandez E, Fernandez MJ, Brana AF, Weissbach U, Kunzel E, Rohr J, Mendez C, Salas JA. Characterization of two glycosyltransferases involved in early glycosylation steps during biosynthesis of the antitumor polyketide mithramycin by *Streptomyces argillaceus*. *Mol. Gen. Genet.* 2000; 262:991–1000. [PubMed: 10660060]



**Figure 1.**

(A) A representative set of angucycline type II polyketides. (B) The previously proposed biosynthesis of BE-7585A based on <sup>13</sup>C labeling studies, with an emphasis on the oxidation reactions.<sup>13</sup> The minimal PKS produces a 20-carbon poly- $\beta$ -ketone that is reduced at the C9 position and cyclized. BexF is proposed to catalyze fourth ring cyclization to produce the linear tetracyclic intermediate that is the substrate for a series of putative oxidation steps. In this work, we propose that a different linear tetracyclic intermediate, 12-deoxy-aklaviketonic acid, is the true BexE substrate. BexE, BexI, and BexM are proposed to form the BE-7585A



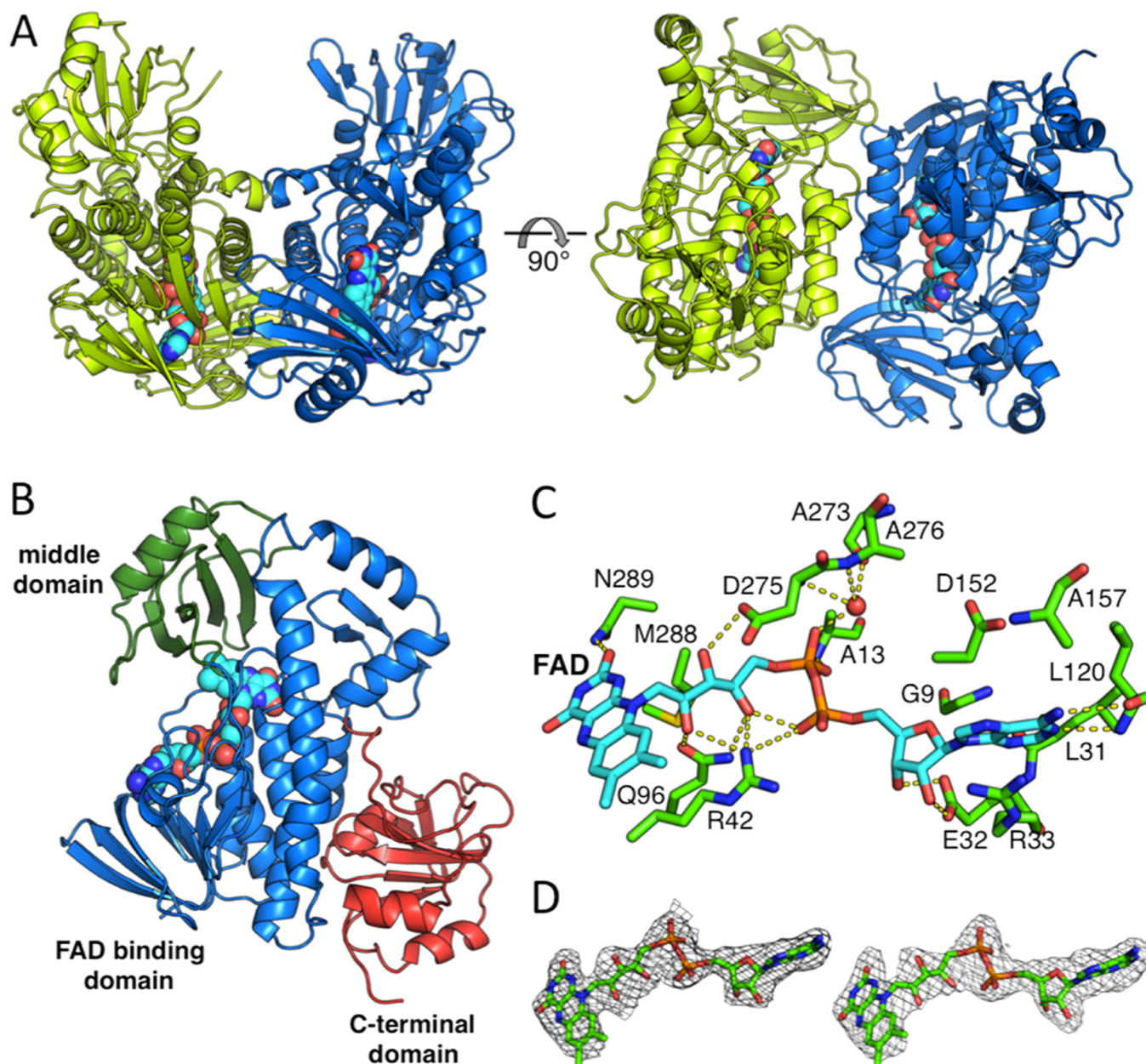
aglycone core, which is further modified by hydroxylation and glycosylation to yield the final product.

Author Manuscript

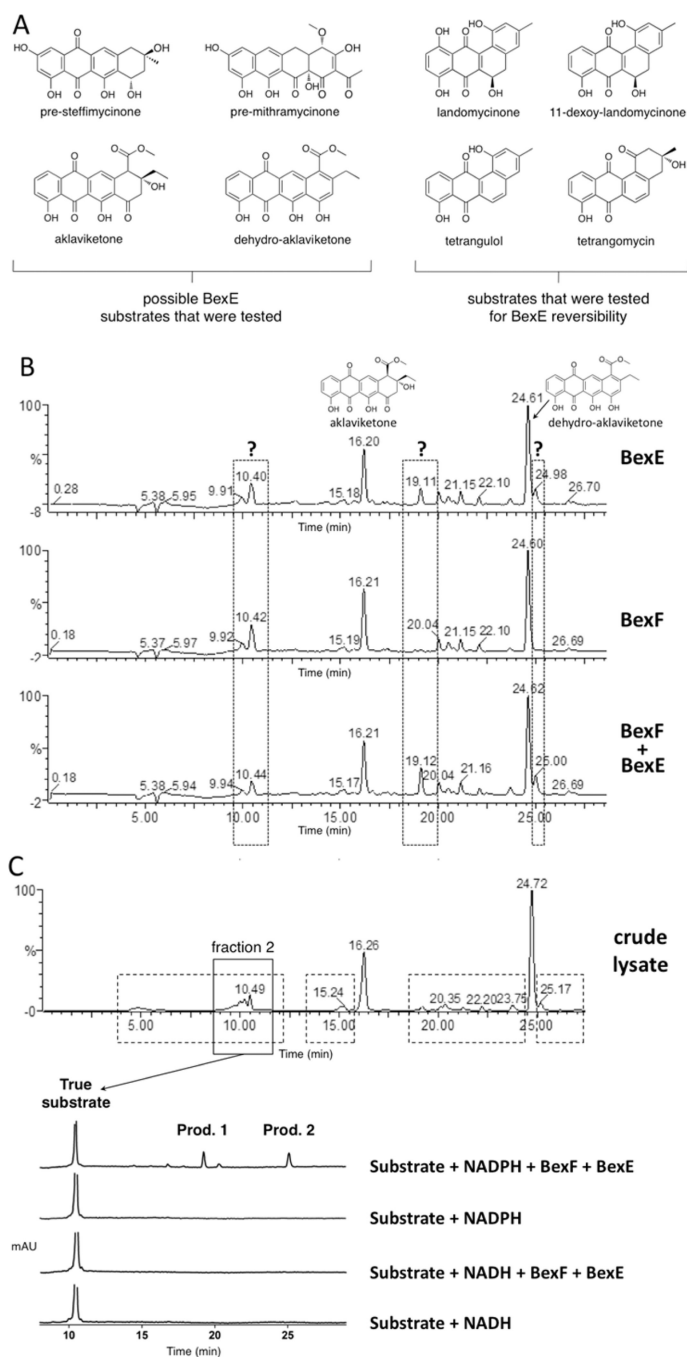
Author Manuscript

Author Manuscript

Author Manuscript



**Figure 2.** Overall structure of the BexE dimer and domain organization of the BexE monomer. (A) The BexE dimer (monomer A in green and monomer B in blue). (B) The BexE monomer is composed of three domains: the FAD binding domain (residues 1–169 and 259–372, colored in blue), the middle domain (residues 170–258, colored in green), and the C-terminal domain (373–487, colored in red). (C) A molecular view of the BexE FAD binding site. (D) SA-Fo-Fc omit map contoured at  $1.5 \sigma$  displaying clear density for FAD in monomer A (left) and monomer B (right).

**Figure 3.**

(A) Possible substrates tested for BexE activity. (B) HPLC analysis of reactions using the *Streptomyces galilaeus* (ATCC 31615) lysate with BexE and BexF. The main products in the lysate are aklaviketone and dehydro-aklaviketone, shown at 16.20 and 24.61 min, respectively. The addition of BexE to the *Streptomyces galilaeus* (ATCC 31615) lysate results in the appearance of two new peaks at 19.11 and 24.98 min. (C) The fractionation of the *Streptomyces galilaeus* (ATCC 31615) lysate to identify the BexE substrate. HPLC was used to fractionate areas with increased peak sizes in the lysate after 5 h of incubation to

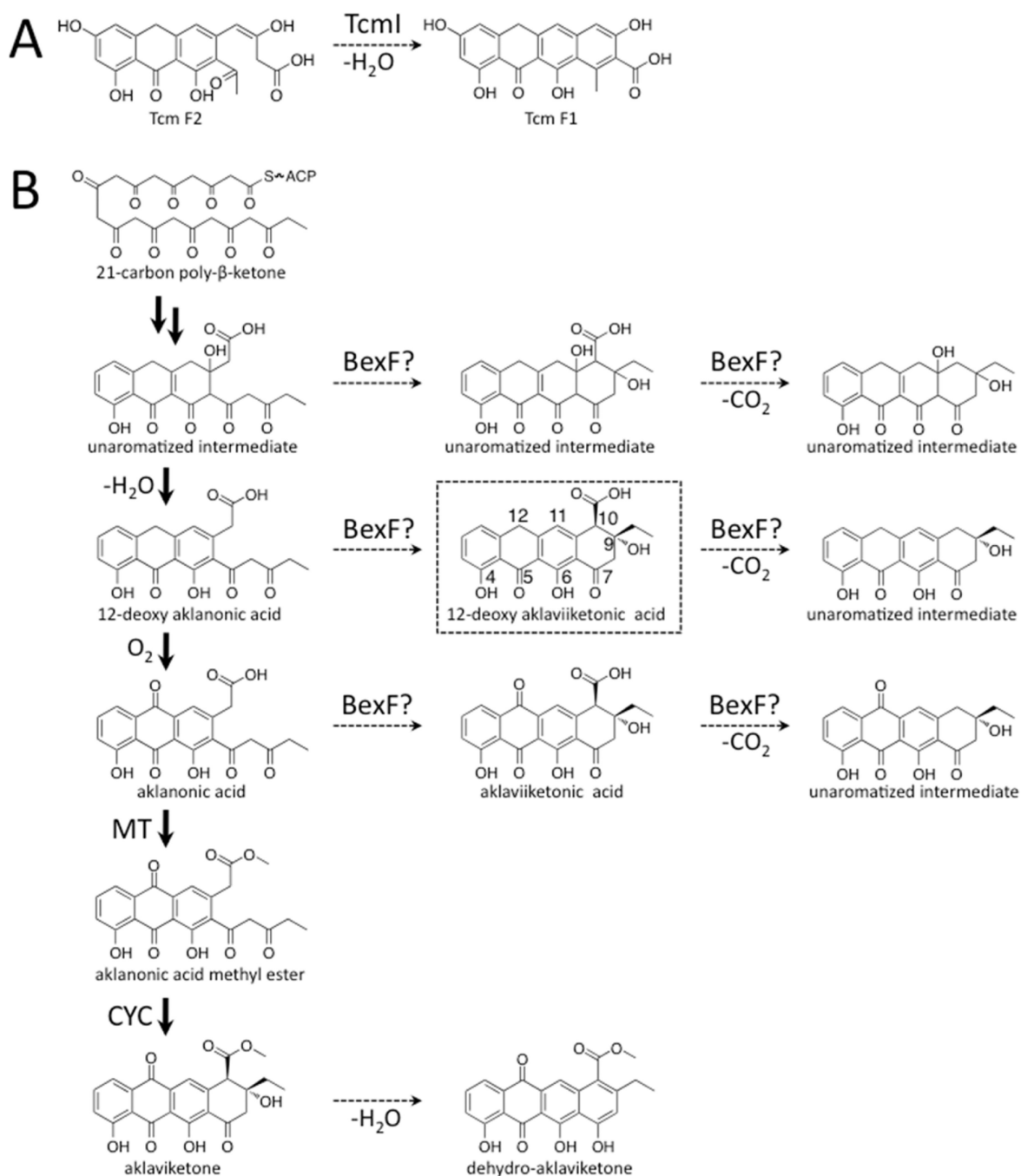
identify the BexE substrate (shown in dotted boxes). Fraction 2 contained a peak at 10.49 min, which contains the true BexE substrate. Fraction 2 was assayed with BexE and BexF in the presence of NADPH or NADH. Assays with the purified fraction 2 confirmed that the BexE reaction is NADPH dependent.

Author Manuscript

Author Manuscript

Author Manuscript

Author Manuscript

**Figure 4.**

Reaction catalyzed by TcmI and type II polyketide biosynthesis of aklaviketone in *Streptomyces galilaeus* (ATCC 31615). (A) TcmI is a fourth ring cyclase from the tetracenomyacin biosynthesis pathway that catalyzes closure of the fourth ring of Tcm F2 to form Tcm F1. (B) Aklaviketone biosynthesis in *Streptomyces galilaeus* (ATCC 31615) follows a linear pathway starting from a 21-carbon intermediate (shown in bold arrows). Many putative intermediates occur transiently during aklaviketone biosynthesis, and we hypothesize that BexF may cyclize an intermediate to form the BexE substrate. Based on

molecular docking studies, we propose that BexF generates 12-deoxy-aklaviketononic acid, which is then used by BexE as a substrate.

Author Manuscript

Author Manuscript

Author Manuscript

Author Manuscript



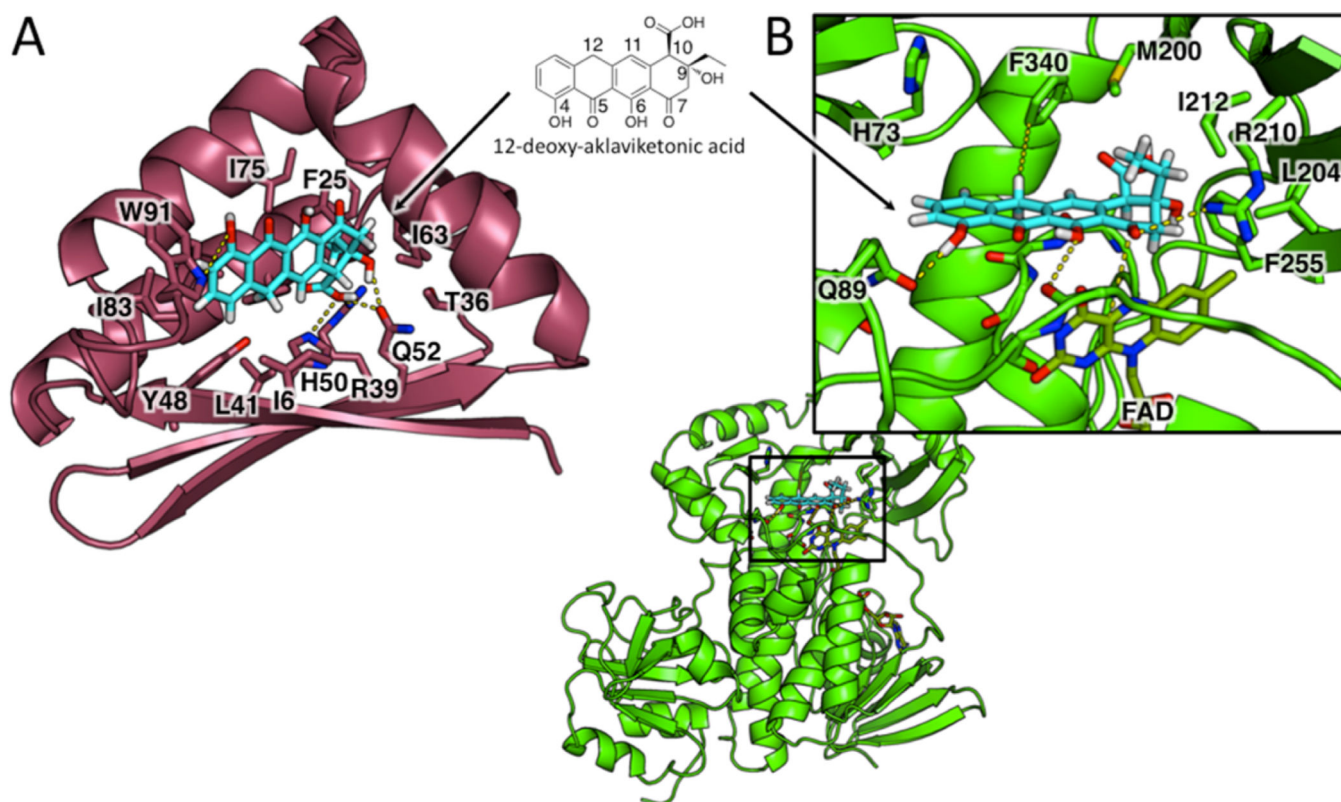


**Figure 5.** Docking of 12-deoxy-aklaviketonic acid into the active sites of the BexF homology model and BexE crystal structure. (A) 12-Deoxy-aklaviketonic acid was docked into the active site pocket of the BexF homology model to determine if this product would engage in favorable interactions with active site residues. 12-Deoxy-aklaviketonic acid docks in the BexF active site and makes favorable hydrophobic and hydrophilic interactions with active site residues. Specifically, the fourth ring of 12-deoxy-aklaviketonic acid is positioned deep in the active site and makes interactions with His50, Arg39, and Gln52. The tetracyclic core sits in a hydrophobic cavity and is anchored by a hydrogen bond between the C4 hydroxyl group and Trp91. (B) 12-Deoxy-aklaviketonic acid was docked into the active site pocket of the BexE crystal structure to determine if this product would engage in favorable interactions with active site residues. 12-Deoxy-aklaviketonic acid docks with the fourth ring close to the C4a carbon of FAD, the site of peroxy-flavin generation. The C4 hydroxyl group of 12-deoxy-aklaviketonic acid is anchored by a hydrogen bond with Gln89. Hydrophobic interactions occur between the hydrophobic side 12-deoxy-aklaviketonic acid and Phe340. Additionally, the propyl moiety of 12-deoxy-aklaviketonic acid forms hydrophobic contacts with Met200, Ile212, and Phe255. Arg210 forms a hydrogen bond with the C7 carbonyl, which may stabilize an oxyanion if this carbonyl undergoes nucleophilic attack by the peroxy-flavin intermediate.



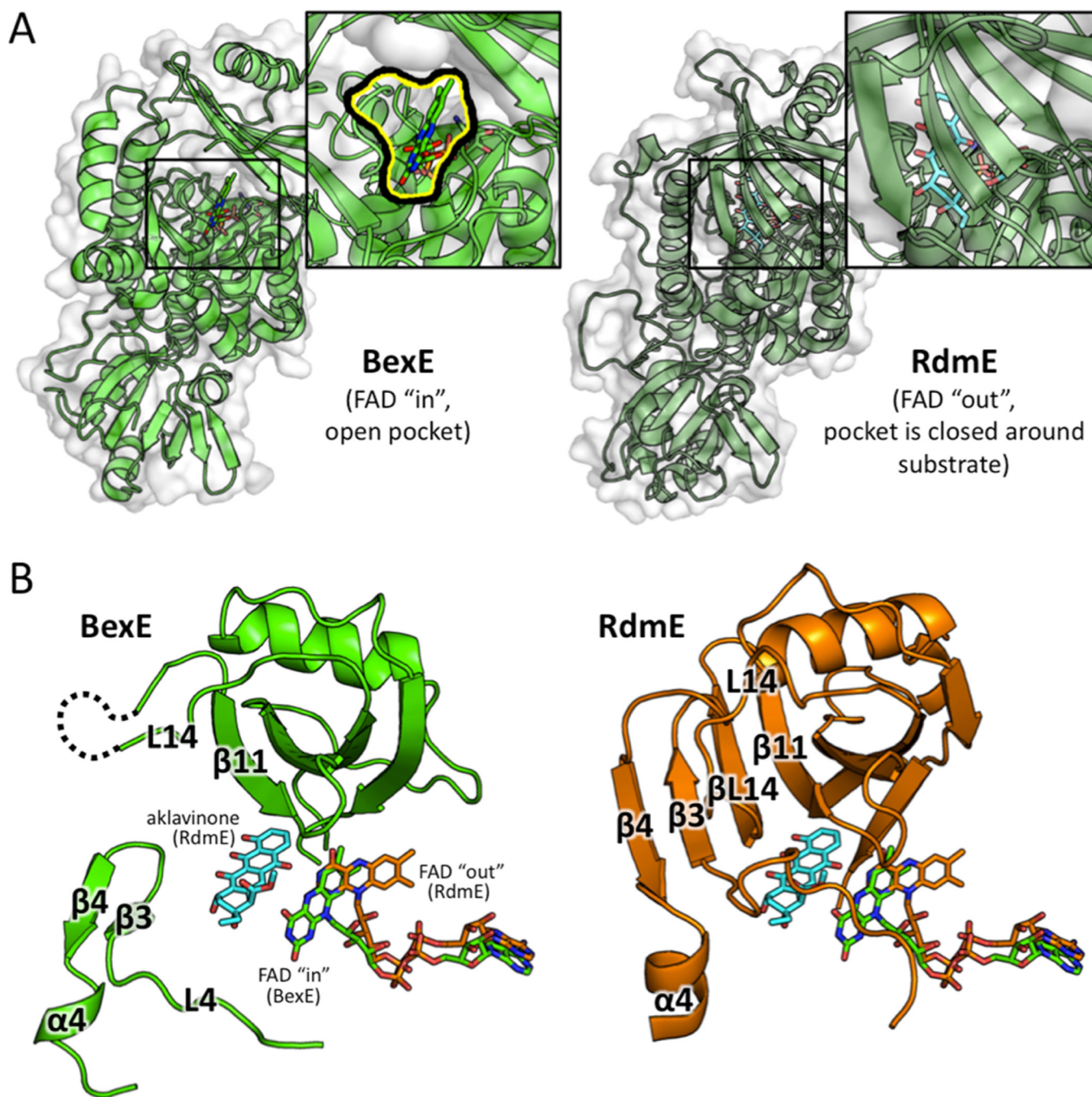


**Figure 6.**

A structural comparison between the middle domains of BexE with FAD in the "in" position and RdmE bound to aklavinone and FAD in the "out" position. (A) BexE with FAD in the "in" position with a zoomed in view of the putative active site entrance (left). RdmE bound to aklavinone with FAD in the "out" position with a zoomed in view of the area corresponding to the BexE active site entrance (right). In RdmE, there is no active site entrance in this area where the substrate is bound. (B) In BexE (left, light green), FAD is in the "in" position with an open active site. The  $\beta$ -hairpin consisting of  $\beta$ 3 and  $\beta$ 4 is relaxed

and shifted downward compared to the same region in RdmE (right, dark green). The L14 region of BexE could not be modeled because of lack of electron density; however, in RdmE this loop forms a  $\beta$ -strand ( $\beta$ L14), which forms a  $\beta$ -sheet with  $\beta$ 3,  $\beta$ 4, and  $\beta$ 11. \*Aklavinone, and FAD from both structures are overlaid in both BexE and RdmE to highlight the FAD motion with respect to substrate position.

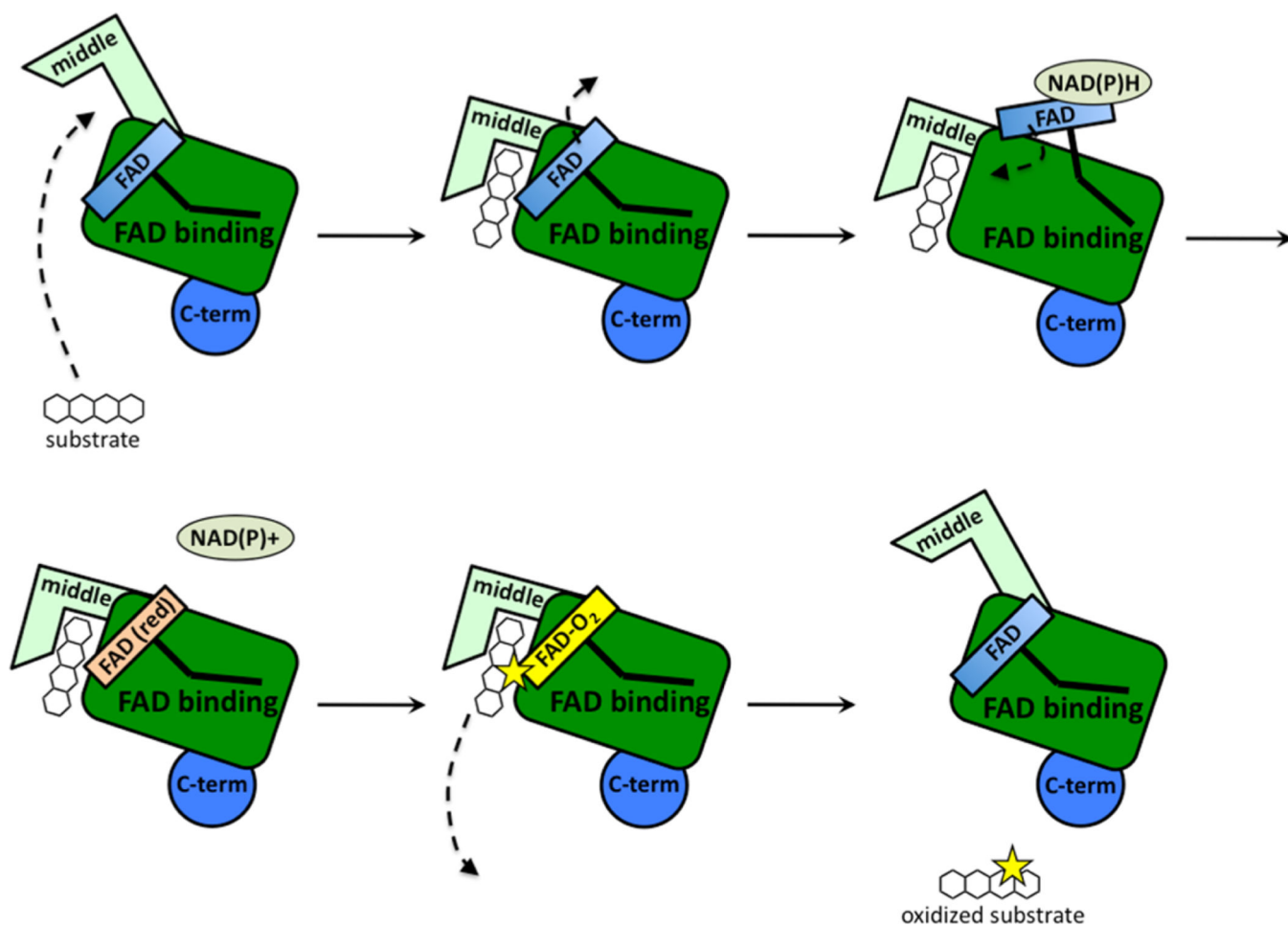


**Figure 7.** Proposed steps during substrate binding and conformational changes in the middle domain during catalysis. Substrate binding induces a conformational change in the middle domain of BexE, which causes FAD to move from the “in” to the “out” position. When FAD is in the “out” position, NADPH reduction occurs and FAD returns to the “in” position. The reduced FAD reacts with molecular oxygen to form a reactive C4a peroxy-flavin intermediate. The reactive C4a peroxy-flavin intermediate delivers oxygen to the substrate and the product is released.